General Base Catalysis in the Urate Oxidase Reaction: Evidence for a Novel Thr−Lys Catalytic Diad †

ARTICLE *in* BIOCHEMISTRY · MAY 2003

Impact Factor: 3.02 · DOI: 10.1021/bi027377x · Source: PubMed

4 AUTHORS, INCLUDING:

Nicholas Power
London South Bank University
18 PUBLICATIONS **594** CITATIONS
SEE PROFILE

Martin Jack Borrok
MedImmune, LLC
16 PUBLICATIONS **346** CITATIONS
SEE PROFILE

General Base Catalysis in the Urate Oxidase Reaction: Evidence for a Novel Thr−Lys Catalytic Diad†

Rebecca D. Imhoff, Nicholas P. Power, M. Jack Borrok, and Peter A. Tipton*

Department of Biochemistry, University of Missouri, Columbia, Missouri 65211

Received December 18, 2002; Revised Manuscript Received February 18, 2003

ABSTRACT: Urate oxidase catalyzes the oxidation of urate without the involvement of any cofactors. The gene encoding urate oxidase from *Bacillus subtilis* has been cloned and expressed, and the enzyme was purified and characterized. Formation of the urate dianion is believed to be a key step in the oxidative reaction. Rapid-mixing chemical quench studies provide evidence that the dianion is indeed an intermediate; at 15 °C the dianion forms within the mixing time of the rapid-quench instrument, and it disappears with a rate constant of 8 s^{-1}. Steady-state kinetic studies indicate that an ionizable group on the enzyme with a p*K* of 6.4 must be unprotonated for catalysis, and it is presumed that the role of this group is to abstract a proton from the substrate. Surprisingly, examination of the active site provided by the previously reported crystal structure does not reveal any obvious candidates to act as the general base. However, Thr 69 is hydrogen-bonded to the ligand at the active site, and Lys 9, which does not contact the ligand, is hydrogen-bonded to Thr 69. The T69A mutant enzyme has a V_{max} that is 3% of wild type, and the K9M mutant enzyme has a V_{max} that is 0.4% of wild type. The ionization at pH 6.4 that is observed with wild-type enzyme is absent in both of these mutants. It is proposed that these residues form a catalytic diad in which K9 deprotonates T69 to allow it to abstract the proton from the N9 position of the substrate to generate the dianion.

Most enzymes that utilize O_2 as a substrate require a cofactor to mediate the chemistry with O_2; urate oxidase is quite unusual in that no cofactor participates in the catalytic reaction. Analytical data as well as the crystal structure of the enzyme from *Aspergillus flavus* have demonstrated that the active enzyme does not contain any transition metals or organic cofactors, nor are there any modified amino acid residues present at the active site (*1*, *2*). The enzyme catalyzes the oxidation of urate to 5-hydroxyisourate; isotope labeling studies have shown that O_2 is reduced to H_2O_2 during the reaction, and the oxygen atom attached to C5 in the product is derived from solvent (*1*, *3*).

A mechanism for the urate oxidase reaction has been proposed in which urate reacts directly with O_2 in a manner analogous to reduced flavin to form a urate hydroperoxide intermediate. Expulsion of H_2O_2 from urate hydroperoxide and hydration of the resulting dehydrourate generates the observed product, 5-hydroxyisourate (Scheme 1). Two intermediates have been detected during single-turnover stopped-flow spectroscopic studies of the enzyme from soybean (*Glycine max*). The first intermediate was assigned to the urate dianion, which is presumed to be the species that reacts directly with O_2. The second intermediate was assigned to the urate hydroperoxide formed from the urate dianion and O_2 (*4*). Model studies using cyclic voltammetry have shown that the peak potential for oxidation of urate decreases with increasing pH, showing that oxidation of the urate dianion is more facile than oxidation of the monoanion

Scheme 1

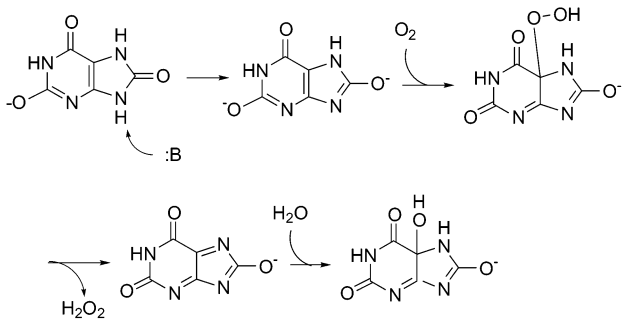

or uric acid (*5*), and it can readily be observed that the rate of nonenzymatic oxidation of urate increases at higher pH. Computational studies have provided insight into these experimental observations. As uric acid undergoes sequential deprotonation, first from N3 and then from N9, electron density accumulates at C5, the site of addition of O_2. Calculations indicate that loss of an electron from the urate dianion is a spontaneous process in the gas phase (*6*).

These observations suggest that a key function for the enzyme in the catalytic reaction is to provide a general base to generate the reactive urate dianion. Indeed, pH kinetic studies of the soybean enzyme indicated that urate binds as the monoanion and that an unprotonated residue on the enzyme is required for catalysis (*1*). However, inspection of the active site in the *A. flavus* enzyme, which contains the competitive inhibitor 8-azaxanthine bound at the active site, does not reveal any obvious candidates for residues that could act as the general base.

† Supported by USDA Grant 2001-35318-10097.

* To whom correspondence should be addressed. Telephone: (573) 882-7968. Fax: (573) 884-4812. E-mail: tiptonp@missouri.edu.

10.1021/bi027377x CCC: $25.00
Published on Web 03/20/2003

We report here the results of site-directed mutagenesis studies that identify the residues involved in the deprotonation of urate. As part of this work, we have also devised a rapid-mixing chemical quench experiment to monitor the lifetime of the urate dianion at the enzyme active site. Our results suggest that an active site lysine and a threonine form a catalytic diad in which the lysine residue deprotonates threonine, allowing the threonine to abstract a proton from the substrate.

MATERIALS AND METHODS

Cloning and Purification of Bacillus subtilus Urate Oxidase. The gene encoding urate oxidase in *B. subtilis* was amplified from genomic DNA using standard PCR techniques. The urate oxidase sequence was obtained from GenBank (accession number Z99120). The forward primer incorporated an *Nde*I site, and the reverse primer contained a *BamH*I site. The amplified product was cloned into the pCRII vector and then excised by digestion with *Nde*I and *BamH*I. The insert was cloned into the expression vector pET-14b to generate a construct that expressed urate oxidase with a $(His)_6$-tag at the N-terminus. Site-directed mutants were constructed using the QuikChange mutagenesis kit (Stratagene). Presumptive mutants were sequenced to verify that no other mutations were introduced during the procedure.

For production of urate oxidase, *Escherichia coli* BL21-(DE3) cells were transformed with the expression plasmid, and cultures were grown at 37 °C in LB media containing ampicillin (100 μg/mL). Six liters of media were inoculated with approximately 300 mL of log phase culture and grown at 25 °C to an OD_{600} of 1. Expression was induced by the addition of IPTG to a final concentration of 0.4 mM, and the cultures were allowed to grow overnight at 25 °C before they were harvested by centrifugation. The cell paste was stored at −80 °C until used.

To purify urate oxidase, 10 g of cell paste was thawed in 40 mL of 50 mM Tris, pH 8.0 containing 2 mM $MgSO_4$, 2 mM $CaCl_2$, 0.5 mM PMSF,[1] and 0.5 mM TLCK. The cells were incubated at 37 °C, and 2 mg of lysozyme and 20 μg of DNaseI were added. After 1 h, the viscous solution was sonicated briefly and centrifuged at 17 500*g* for 45 min. The pelleted cell debris was discarded.

Nucleic acids in the supernatant were removed by the addition of protamine sulfate. A total of 30 mg of protamine sulfate was added dropwise from a 10 mg/mL stock solution prepared in water. The cell-free extract was stirred on ice during the addition of protamine sulfate and stirred for an additional 15 min after the addition was complete. The solution was centrifuged at 15 000*g* for 15 min, and the pellet was discarded.

Crystalline ammonium sulfate was added to 30% saturation, and the solution was centrifuged at 15 000*g* for 15 min. The pellet was discarded, and the supernatant was raised to 55% saturation by the addition of solid ammonium sulfate. The solution was centrifuged as above; the supernatant was discarded, and the pellet was dissolved in 20 mM sodium phosphate, pH 7.4, containing 10 mM imidazole and 0.5 M NaCl (buffer A).

A Fast Flow Chelating Sepharose column was charged with Ni^{2+} according to the manufacturer's instructions (Pharmacia) and equilibrated in buffer A. Purity and yield were optimal when the column contained 1 g of resin per 10 mg of protein. Buffer B consisted of buffer A with the addition of 140 mM imidazole, and buffer C was identical except the concentration of imidazole was 500 mM. The protein solution was loaded onto the column and washed with 7.5 volumes of buffer A. The resin was then washed with 7.5 volumes of buffer B and finally 7.5 volumes of buffer C. The fractions were assayed for the presence of urate oxidase by the spectrophotometric assay described below and by SDS−PAGE. Active fractions were pooled and desalted with a BioRad Bio-Gel P-6 DG desalting column equilibrated in 10 mM Tris pH 8.0 containing 100 mM NaCl.

Purified proteins were stored at 4° in Tris buffer containing 10% glycerol. The CD spectra of all mutant proteins were obtained and compared to wild-type, to ensure that the mutant proteins were folded properly.

Urate Oxidase Assays. Urate oxidase activity during the purification was measured spectrophotometrically by monitoring the disappearance of urate at its absorbance maximum at 292 nm. Standard assay conditions were 50 mM Tris, pH 8.0, and 0.1 mM urate. The simple spectrophotometric assay provides qualitative estimates of enzyme activity but suffers from the fact that the product of the reaction, 5-hydroxyisourate, has significant absorption at 292 nm; since it is a relatively unstable species, its concentration changes in a complex way during the course of the reaction, complicating the extraction of rate data from the absorbance timecourse. To obtain accurate kinetic data for reactions in which the HIU concentration could not be discounted, the reactions were monitored by measuring the concentration of H_2O_2 in aliquots removed at discrete time points. H_2O_2 concentrations were determined colorimetrically based on the formation of an Fe^{3+}−xylenol orange complex (*7*). The reagents for the colorimetric assay are 25 mM $(NH_4)_2Fe(SO_4)_2$ in 2.5 M H_2SO_4 and 125 μM xylenol orange in H_2O, which are combined in the ratio 1:100 immediately before use. A 100 μL aliquot of the enzymatic reaction was added to the combined reagents, and color development was allowed to proceed at room temperature for 15 min. The absorbance was read at 560 nm, and the H_2O_2 concentration was determined by comparison with a standard curve generated with authentic H_2O_2. For the pH kinetics studies, the following buffers were used in the pH intervals indicated: MOPSO, pH 5.75−6.25; MES, pH 6.25−6.5; and HEPES, pH 6.5−8.0. Data describing the pH dependence of V and V/K for the wild-type urate oxidase were fitted to eq 1, where C is the pH-independent value of the kinetic parameter.

$$\log Y = \log\left(\frac{C}{1 + H/K_a}\right)$$

Rapid-Mixing Chemical Quench Studies. Single-turnover experiments were performed using a KinTek RQF rapid-mixing instrument thermostated at 15 °C. One substrate syringe contained 250 μM urate oxidase, and the other contained 50 μM [8-^{14}C]urate. The [8-^{14}C]urate was obtained from American Radiolabeled Chemicals and was purifed by

[1] Abbreviations: HEPES, *N*-2-hydroxyethylpiperazine-*N*′-2-ethane sulfonic acid; HIU, 5-hydroxyisourate; MES, 2-(*N*-morpholine)ethane sulfonic acid; MOPSO, 3-(*N*-morpholino)-2-hydroxypropane sulfonic acid; PMSF, phenylmethanesulfonyl fluoride; TLCK, *N*α-*p*-tosyl-L-lysine chloromethyl ketone; UO, urate oxidase.

```
B. subtilis     ---------MKRTMSYGKGNVFAYRTYLKPLTGVKQIPESSFAGRDNTVVGVDVTCEIGG
A. flavus       --------SAVKAARYGKDNVRVYKVHKDEKTGVQTVYEMTVC------VLLEGEIET--
G. max          MAQQEVVEGFKFEQRHGKERVRVARVWKTR-QGQHFVVEWRVG------ITLFSDCVN--
                         **  *   .      * . . *          . .

B. subtilis     EAFLPSFTDGDNTLVVATDSMKNFIQRHLASY-EGTTTEGFLHYVAHRFLDTYSHMDTIT
A. flavus       -----SYTKADNSVIVATDSIKNTIYITAKQN-PVTPPELFGSILGTHFIEKYNHIHAAH
G. max          -----SYLRDDNSDIVATDTMKNTVYAKAKECSDILSAEDFAILLAKHFVSFYKKVTGAI
                     *.   **. .****..** .            * *   .  .*.  * ..

B. subtilis     LTGEDIPFEAMPAYEEKELSTSRLVFRRSRNERSRSVLKAERSGNTITITEQYSEIMDLQ
A. flavus       VNIVCHRWTRMDIDGKP---HPHSFIRDSEEKRNVQVDVVEGKG-----IDIKSSLSGLT
G. max          VNIVEKPWERVIVDGQP---HEHGFKLGSE-KHTTEAIVQKSGS-----LQLTSGIEGLS
                ..       .          .    *   .                    * .  *

B. subtilis     LVKVSGNSFVGFIRDEYTTLPEDGNRPLFVYLNISWQYENTNDSYASD---PARYVAAEQ
A. flavus       VLKSTNSQFWGFLRDEYTTLKETWDRILSTDVDATWQWKNFSGLQEVRSHVPKFDATWAT
G. max          VLKTTQSGFVNFIRDKYTALPDTRERILATEVTALWRYSYESQYSLPQKPFYFTEKYQEV
                ..* .   * .*.** **.* .   * *   .   *.

B. subtilis     VRDLASTVFHELE----TPSIQNLIYHIGCRILARFPQLTDVSFQSQN-HTWDTVVEEIP
A. flavus       AREVTLKTFAEDN----SASVQATMYKMAEQILARQQLIETVEYSLPNKHYFEIDLSWHK
G. max          KKVLADTFFGPPNGGVYSPSVQNTFYLMAKATLNRFPDIAYVSLKMPNLHFLPVNISNKD
                 . ..   *        . *.*   * .    * *   .  *     * *     .

B. subtilis     G-----SKGKVYTEPRPPYGFQHFTVTREDAEKEKQKAAEKCRSLKAZ
A. flavus       GLQNTGKNAEVFAPQSDPNGLIKCTVGRSSLKSKL-------------
G. max          G-PIVKFEDDVYLPTDEPHGSIQASLSR--LWSKLZ------------
                *        *.    * *  . .. *
```

FIGURE 1: Sequence alignment of urate oxidases from *B. subtilis*, *A. flavus*, and *G. max* (soybean). The residues that are shown in boldface are Phe 159, Arg 176, and Gln 228 (*A. flavus* numbering), which are observed in the crystal structure to interact with 8-azaxanthine at the active site and Lys 10, Thr 57, and Asp 58, whose roles have been explored by mutagenesis in this work.

HPLC, as described below, before use. Rapid-quench experiments were conducted using two different quench reagents, methanol and 1 M HCl. The quenched samples were lyophilized, redissolved in 0.1 mL of 5 mM sodium phosphate, pH 4.4, and centrifuged briefly. Each sample was analyzed by HPLC using an Asahipak GS-320HQ column (Shodex). The column was equilibrated in 5 mM sodium phosphate, pH 4.4, and run at a flow rate of 0.5 mL/min. Samples (0.1 mL) were injected and monitored by absorbance at 225 nm. The effluent was collected in 0.25 mL fractions; to each fraction 5 mL of Scintiverse BD was added, and the fractions were counted with a Beckman LSC 6000 liquid scintillation counter.

RESULTS

B. subtilis Urate Oxidase Cloning and Purification. The studies presented in this report have been conducted with urate oxidase from *B. subtilis*; the bacterial enzyme is far more soluble than the soybean enzyme we have studied earlier and thus more amenable to experimental methods that require high protein concentrations. The enzymes share considerable sequence identity, and the data we have obtained suggest that there are no qualitative differences in the chemical mechanisms of the enzymes from the two sources.

The gene encoding urate oxidase was found as a GenBank entry that was annotated as the *yunL* gene, with unknown function. The homology with urate oxidase genes from diverse species was readily apparent, however (*8*). The resulting gene codes for a protein containing 325 amino acids with a calculated molecular weight of 38 611 Da. The extent of the conservation of amino acids between the proteins from *B. subtilis*, soybean, and *A. flavus* was only moderate. The pairwise identity between the *B. subtilis* UO and soybean UO was 25% over 224 residues; between *B. subtilis* UO and *A. flavus* UO was 29% over 211 residues; and between soybean UO and *A. flavus* UO was 36% over 241 residues. However, all of the amino acid residues that are observed to interact with the substrate analogue in the active site of *A. flavus* UO, as well as the residues that were investigated in the present study by mutagenesis, are strictly conserved (Figure 1).

The expressed protein showed the expected urate oxidase activity and was readily purified to homogeneity using ammonium sulfate precipitation and immobilized metal ion chromatography. The purified protein could be concentrated to 15 mg/mL without precipitating, in contrast to the soybean enzyme that can be concentrated to 1 mg/mL only with difficulty. With air-saturated buffer the K_m for urate was 34 μM, and V_{max} was 3.3 s^{-1}. Under these conditions, the soybean enzyme is characterized by a K_m for urate of 21 μM and V_{max} of 5.9 s^{-1}.

Kinetic Properties of Mutant Enzymes. Three amino acid residues in the active site were selected for mutational analysis, D70, T69, and K9. The kinetic properties of the mutant enzymes that were constructed are listed in Table 1. The CD spectra of the mutant proteins were not different from the CD spectrum of the wild-type enzyme (data not shown).

The pH dependence of the kinetic parameters V and V/K for the wild-type *B. subtilis* urate oxidase and for two mutant proteins, T69A and K9M, are shown in Figure 2. For the wild-type enzyme, both V and V/K were pH dependent, with

Table 1: Steady-State Kinetic Parameters of *B. subtilis* UO Mutants

enzyme	V_{max} (s^{-1})	K_m (μM)	V/K ($\mu M\ s^{-1}$)
wild type	3.26 ± 0.12	34 ± 5	0.097 ± 0.015
D70A	2.10 ± 0.06	28 ± 3	0.075 ± 0.008
T69A	0.099 ± 0.003	170 ± 13	$5.8 \pm 0.5 \times 10^{-4}$
K9M	0.0135 ± 0.0003	51 ± 4	$2.6 \pm 0.2 \times 10^{-4}$
T69V	0.0198 ± 0.0006	1050 ± 120	$1.9 \pm 0.2 \times 10^{-5}$
T69A/K9M	0.036 ± 0.0004	547 ± 28	$6.6 \pm 0.3 \times 10^{-5}$

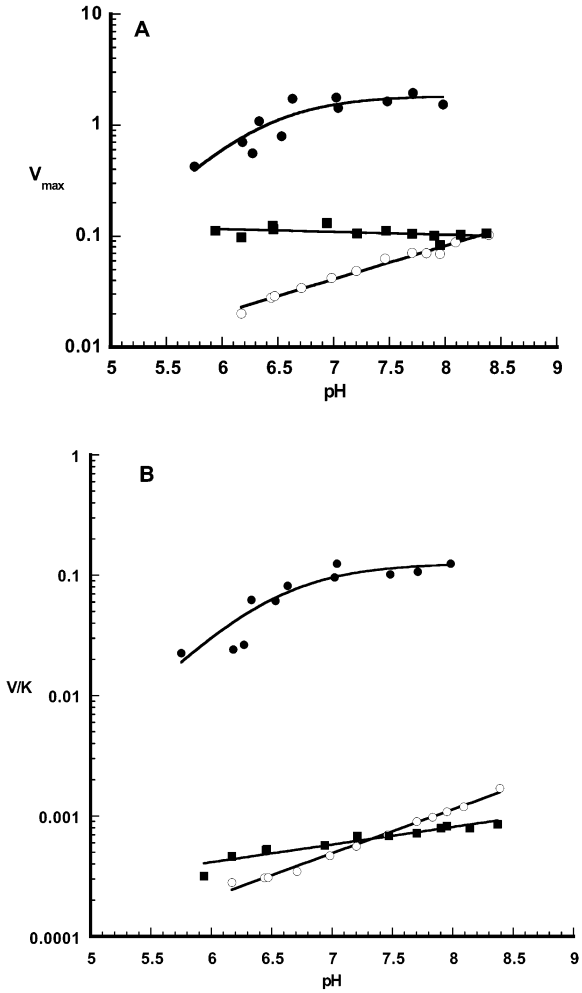

FIGURE 2: Steady-state kinetic parameters for the urate oxidase-catalyzed oxidation of urate as a function of pH. Wildtype (●); T64A (■); and K9M (○). (A) V_{max}. (B) V/K. The experimental points for the wild-type enzyme were fitted to eq 1. The experimental points for the mutants were fitted to an exponential function (note the log scale).

both parameters decreasing below a pK of about 6.5. No pK was evident in the pH profiles of the mutant enzymes, although V and V/K showed a modest, linear dependence on pH.

Rapid-Mixing Chemical Quench Experiments. Quenching the urate oxidase reaction with methanol resulted in a mixture of products (Figure 3). Allantoin and urate eluted from the HPLC column at 31 and 66 min, respectively. The decomposition of 5-hydroxyisourate and intermediates that were present in the sample at the time of the quench resulted in one major product that eluted at 35 min and several minor products; no attempt was made to identify those species. The samples quenched with acid and MeOH yielded similar chromatograms, except for differences in the relative amounts

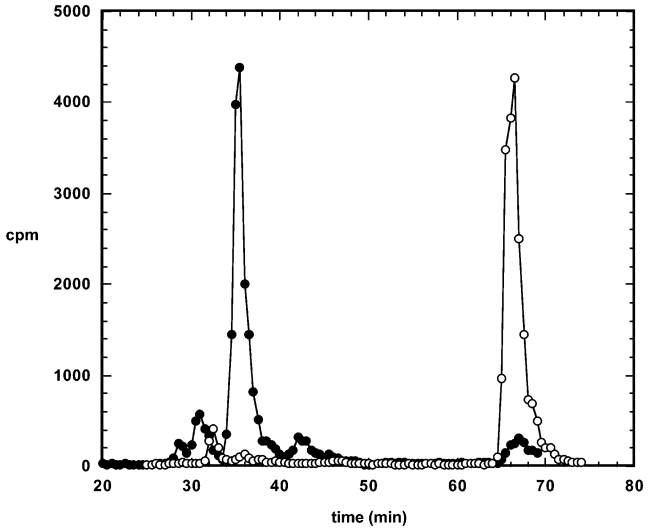

FIGURE 3: Separation of components from the quenched urate oxidase reaction. The samples shown were quenched after 10 ms of reaction. The components were separated by HPLC using an Asahipak GS320-HQ column, as described in the text. Methanol quench, (●) and HCl quench, (○). Comparison with authentic samples established that urate elutes at 66 min and allantoin elutes at 31 min.

of urate and the decomposition products. The intermediates that form during the catalytic cycle, as well as the product itself, 5-hydroxyisourate, are unstable and decompose in methanol or acidic solutions, but urate is stable under these conditions. Control experiments established that the urate dianion is not stable in methanol; however, when the enzymatic reaction is quenched with acid, the urate dianion that is present is simply protonated to form uric acid, which is stable. Thus, the amount of the urate dianion that is present at any point in time during the urate oxidase reaction can be determined by subtracting the amount of urate present in the methanol quench samples (which is unreacted urate) from the amount of urate present in the acid quench samples (which is the sum of the unreacted urate and the urate formed from protonation of the urate dianion). Figure 4 shows the time dependence of the urate concentration in the methanol and acid quench experiments. The time course for the urate dianion is the difference between these experimental points and is also shown in Figure 4. The calculated points describe a first-order decay with a rate constant of $8 \pm 1\ s^{-1}$.

DISCUSSION

The urate oxidase reaction proceeds without the participation of any cofactor; stopped-flow spectroscopic studies and trapping experiments have provided evidence for the formation of a urate hydroperoxide intermediate during the course of the reaction (*4*, *9*). Model studies have demonstrated that the urate dianion undergoes oxidation very readily, and computational studies show that electron density accumulates at C5 in the urate dianion and that loss of an electron is spontaneous in the gas phase. Thus, an effective catalytic strategy for the enzyme would be to generate the urate dianion at the active site in the presence of O_2; the formation of urate hydroperoxide would be expected to proceed smoothly because of the intrinsic reactivity of the urate dianion.

Studies of the pH dependence of the steady-state kinetic parameters have suggested that urate binds to the soybean

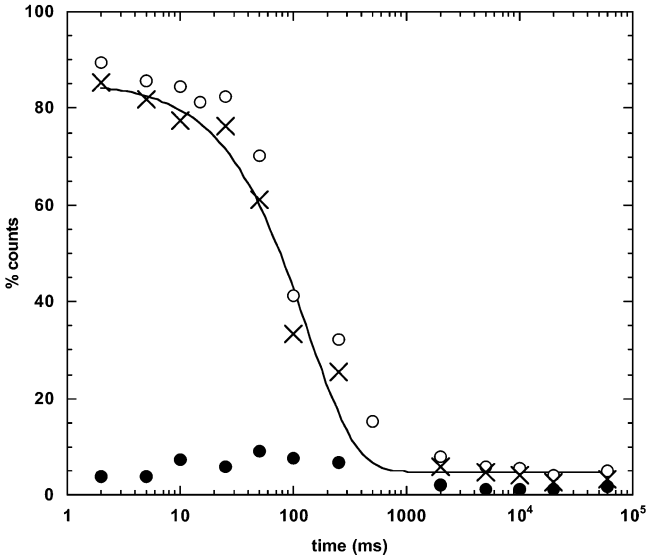

FIGURE 4: Time course for the urate oxidase reaction under single turnover conditions. The experimental points are the amount of urate detected in the HCl quench (○) and the methanol quench (●). The amount of urate dianion calculated at each time point is indicated by (×); the solid line is the fit of the calculated urate dianion time points to a single exponential.

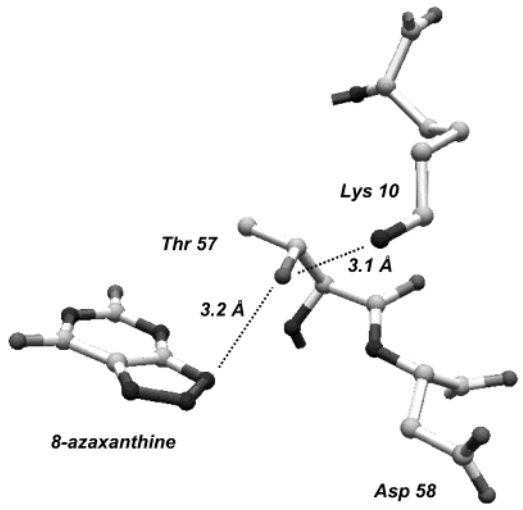

FIGURE 5: Active site of *A. flavus* urate oxidase. The residues that were mutated in this investigation are indicated. *A. flavus* K10, T57, and D58 correspond to residues K9, T69, and D70 in *B. subtilis* urate oxidase. The *A. flavus* urate oxidase structure is deposited in the PDB under the code 1UOX.

enzyme as the monoanion; furthermore, an ionizable group on the soybean enzyme with a p*K* of 6.4 must be unprotonated for the catalytic reaction to proceed (*1*). Thus, it is attractive to propose that the active site contains an amino acid residue that acts as a general base to abstract a proton from the urate monoanion to generate the reactive dianion.

To establish in a more direct manner whether urate dianion forms during the catalytic cycle, we turned to transient-state kinetic studies. Rapid-mixing chemical quench studies establish that highly reactive intermediates form during the catalytic cycle (Figure 3). Significantly, the amount of urate that was present in the quenched samples differed dramatically depending on whether the reactions were quenched with methanol or acid. In methanol-quenched samples, urate was almost completely absent in even the earliest timepoints, whereas urate was present in samples quenched after several hundred milliseconds in the acid-quenched reactions. The simplest interpretation of these data is that an intermediate forms during the catalytic reaction that is unstable in methanol but that can form urate under acidic conditions. This intermediate is presumed to be the urate dianion. Control experiments confirmed that the urate dianion decomposed upon addition to methanol to yield primarily the species that elutes at 35 min; upon addition to acidic solution, the dianion is simply protonated to form uric acid.

The amount of urate that is present in the acid-quenched samples is the sum of the urate that has not yet reacted, and the urate that was present on the enzyme as the dianion that was reprotonated when the reaction was quenched. The urate in the methanol-quenched samples arises only from the urate that has not yet reacted. Therefore, the amount of urate dianion that is present at any point in time during the catalytic cycle can be calculated by subtracting the amount of urate present in the methanol-quenched sample from the amount of urate present in the acid-quenched sample (Figure 4). The timecourse for urate dianion, thus calculated, decays with a first-order rate constant of 8 s^{-1} at 15 °C. Since V_{max} at 25 °C is 3.3 s^{-1}, the urate dianion is clearly a kinetically competent intermediate. Urate dianion formation apparently occurred within the mixing time of the instrument because even in experiments conducted at 5 °C the dianion concentration was maximal at the earliest timepoints. Stopped-flow spectroscopic studies of the soybean urate oxidase have suggested that decomposition of urate hydroperoxide is largely rate-determining in the overall reaction, and the rate constant for formation of urate dianion at 25 °C was estimated to be >60 s^{-1} (*4*).

The active site of urate oxidase was examined to identify the residue that acts as a general base in the catalytic reaction. Structural information is available only for urate oxidase from the fungus *A. flavus* (*2*); however, the primary sequences of urate oxidases from diverse organisms are known, and signficant conservation of residues throughout the sequence is evident. In particular, the residues that make up the active site in *A. flavus* urate oxidase are also present in the soybean enzyme and the *B. subtilis* enzyme (Figure 1). We have characterized the catalytic reaction of the soybean enzyme in earlier work, but all attempts to generate site-directed mutants resulted in the formation of insoluble protein. We therefore cloned and expressed the gene for urate oxidase from *B. subtilis*. The expressed protein was soluble up to ~15 mg/mL, and mutant proteins could be prepared and characterized. The pH dependence of the kinetic parameters was similar to that observed for the soybean enzyme; both V_{max} and V/K decrease with decreasing pH, defining a p*K* of about 6.4. Since the p*K* of the first ionizable site on urate itself is 5.8, the p*K* observed in the pH profiles is presumed to arise from the ionization of a residue on the protein.

Inspection of the *A. flavus* UO active site does not suggest obvious candidates for the ionizable residue (Figure 5). Among the amino acids that are commonly considered to be ionizable, Asp 58 (corresponding to Asp 70 in the *B. subtilis* enzyme) is the only one present at the active site. Its carboxyl group is directed away from the active site ligand; however, rotation around a single bond in the side chain would place the carboxyl group in an appropriate position to abstract a proton from N9 of urate. However,

FIGURE 6: Overlay of the active sites and adjacent structural elements of urate oxidase (purple; PDB code 1uox), 7,8-dihydroneopterin aldolase (yellow; PDB code 2dhn), and GTP cyclohydrolase (red; PDB code 1a8r). The conserved Gln/Glu residues and the active site ligands are shown in ball-and-stick.

mutation of Asp 70 to alanine in *B. subtilis* UO had no significant effect on the kinetic properties of the enzyme, demonstrating that it does not act as a general base in the reaction.

The only other residue evident in the crystal structure that is appropriately positioned to play a role as a general base is Thr 57. The corresponding residue in the *B. subtilis* enzyme is Thr 69 and indeed, V_{max} was decreased significantly in the T69A mutant enzyme. One would not expect threonine to be ionized under most conditions, and neutral threonine could not act as a general base. However, the ϵ amino group of Lys 10 is located 3.1 Å away from the hydroxyl group of Thr 57 in the *A. flavus* enzyme. This lysine residue is conserved in *B. subtilis* UO as Lys 9. Mutation of Lys 9 to a methionine residue demonstrates that it plays a critical role in the catalytic reaction; V_{max} in the K9M mutant was 0.4% that of the wild type. Thus, K9 and T69 may function as a unit in which K9 abstracts a proton from T69, which is then activated to abstract a proton from the substrate. The activity of the double mutant K9M/T69A, as measured by V_{max}, differed only 2−3-fold from the single mutants. This finding is reminiscent of the mutational analysis of the catalytic triad of subtilisin, which revealed that the residues acted synergistically, so that double and triple mutant enzymes had essentially the same activity as the single mutants (*10*). Although V_{max} was not significantly affected by the double mutation, the K_m for urate was substantially increased, suggesting that proper binding of urate was perturbed by the mutations.

The assignment of the ionization defined by the pK of 6.4 in the pH profiles to K9 and T69 is substantiated by the absence of any clearly defined ionization in the pH profiles of the T69A and K9M mutant enzymes. The pH profiles for the K9M mutant are essentially pH-independent; however, in the T69A mutant V_{max} and V/K both increase by about 0.3 log units per pH unit. The origin of this behavior is unclear; if the reaction were arising solely from the amount of urate dianion present in solution or from hydroxide acting as a specific base catalyst, the plots should have unit slopes.

The residual activity in the T69A mutant is not negligible. The crystal structure of the *A. flavus* enzyme shows a water molecule that is positioned 2.8 Å from T69 on the same face of the planar ligand; we hypothesized that perhaps in the absence of Thr 69 the water molecule occupies the vacated space and assumes the role of the threonine hydroxyl group. The T69V mutant was constructed to test that idea since valine is isosteric with threonine. However, V_{max} in the T69V mutant enzyme was only 5-fold lower than in the T69A mutant; a much more dramatic effect on K_m for urate was evident, suggesting that the threonine hydroxyl group participates in hydrogen-bonding interactions that are critical for optimal substrate binding. We are left without a rigorous explanation for the residual activity of the enzyme in the

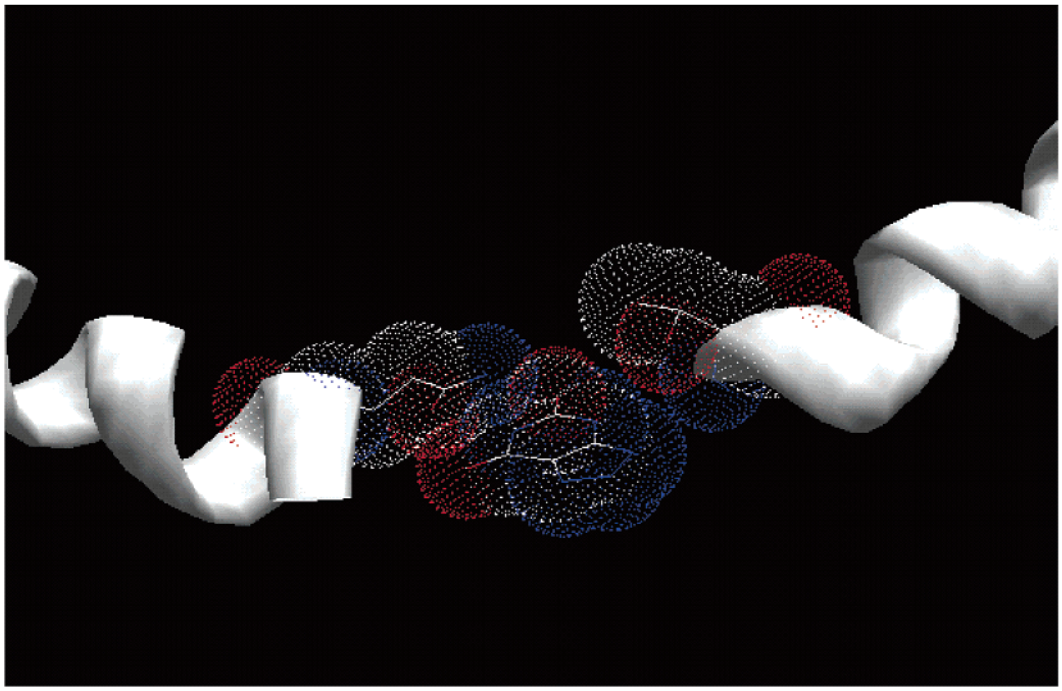

FIGURE 7: 8-Azaxanthine bound at the active site of urate oxidase. The van der Waals surfaces of the ligand, Glu 228, and Thr 57 are indicated.

absence of Thr 69; however, since the p*K* for the proton on N9 of urate is ~10.5, it is not unreasonable to expect that the reaction could proceed slowly in the absence of general base catalysis. Nonenzymatic ionization of urate may also account for the residual activity of the K9M mutant.

The threonine−lysine diad suggested by the mutational data to function as the general base catalyst in the urate oxidase reaction is unusual. However, a similar situation may occur in UDP-galactose 4-epimerase, in which it is not clear whether a tyrosine residue acts directly as the general base or if the tyrosine activates a serine residue to abstract a proton from the substrate (*11*). We searched for other enzymes that may also use a threonine−lysine diad using the program SPASM (*12*). SPASM utilizes a specific protein substructure as a search query and returns proteins that also contain that substructure. The PDB was searched using the T57, K10 residues of *A. flavus* urate oxidase as the search query. A 0.5 Å RMS deviation from the query structure was allowed, and the search returned 56 proteins that contained a threonine−lysine pair in approximately the same geometrical arrangement as *A. flavus* urate oxidase. Of these hits, 39 were enzymes, and they were examined further. However, inspection of the crystal structures did not reveal any obvious instances in which the threonine−lysine diad could be acting as a general base catalyst.

A possible explanation for why threonine is found in its unusual role in UO comes from consideration of the architecture of the enzyme. UO is a homotetramer containing four identical active sites that are found at the interfaces between adjacent subunits. Each subunit consists of two T-domains, a unique fold that, except for UO, is found only in enzymes in the pterin biosynthetic pathway, including GTP cyclohydrolase (*13*), 7,8-dihydroneopterin aldolase (*14*), 6-pyruvoyl tetrahydropterin synthase (*15*), and 7,8-dihydroneopterin triphosphate epimerase (*16*). The pterin biosynthetic enzymes do not share significant sequence homology with each other or with UO. However, as has been noted before (*2*, *16*), the architecture of the T-fold is remarkably well-conserved; the program TOP (*17*) reveals that the Cα positions of UO domain 1 align with GTP cyclohydrolase over 130 residues with an RMS deviation of 1.9 Å; with 6-pyruvoyl tetrahydropterin synthase over 93 residues with an RMS deviation of 1.8 Å; and with 7,8-dihydroneopterin aldolase over 86 residues with an RMS deviation of 1.6 Å. A significant determinant for substrate binding in the pterin biosynthetic enzymes is a conserved glutamate residue that forms two hydrogen bonds with the substrate, one to the amino group at C2, and the other to N1. In *A. flavus* urate oxidase, Gln 228 occupies the equivalent position and forms hydrogen bonds to the C2 carbonyl oxygen and N1 of the ligand at the active site. Using the conserved Glu/Gln as a marker, the active sites of UO and the pterin biosynthetic enzymes can be compared (Figure 6). In UO, Gln 228 from subunit A hydrogen bonds to the ligand at the active site, and Thr 57 is contributed by subunit D, which lies at the N-terminus of a short α-helix. Both the helix that contributes the Glu/Gln and the helix that contributes Thr 57 in the case of UO are remarkably well-conserved in the T-fold domain enzymes; in each instance the helices are on separate subunits. In UO, Thr 57 nestles against the substrate in the position required for proton abstraction; indeed, it appears that a larger residue, even an aspartate, could not be accommodated without disrupting the binding of the substrate (Figure 7). Thus, the adoption of threonine as a general base may be a consequence of the structural motif from which urate oxidase is constructed. Thr 57 is not conserved in any of the pterin biosynthetic enzymes, nor would one expect it to be, since those enzymes carry out chemistry that is unrelated to the urate oxidase reaction. Thr 57 cannot act as a general base unless it is activated by another residue; thus, Lys 10 appears to be appropriately positioned to deprotonate the threonine hydroxyl. It is noteworthy that Lys 10 is within hydrogen-bonding distance of His 256, which appears to be solvent accessible; Thr 57, Lys 10, and His 256 may form a conduit for transferring a proton from the substrate to solvent.

ACKNOWLEDGMENT

We are grateful to Professor Lesa Beamer for performing the SPASM and TOP analyses and for helpful discussions.

REFERENCES

1. Kahn, K., and Tipton, P. A. (1997) *Biochemistry 36*(16), 4731−4738.
2. Colloc'h, N., El Hajji, M., Bachet, B., L'Hermite, G., Schiltz, M., Prange, T., Castro, B., and Mornon, J. (1997) *Nat. Struct. Biol. 4*, 947−952.
3. Kahn, K., Serfozo, P., and Tipton, P. A. (1997) *J. Am. Chem. Soc. 119*, 5435−5442.
4. Kahn, K., and Tipton, P. A. (1998) *Biochemistry 37*, 11651−11659.
5. Goyal, R. N., Mittal, A., and Agarwal, D. (1994) *Can. J. Chem. 72*, 1668−1674.
6. Kahn, K. (1999) *Bioorg. Chem. 27*, 351−362.
7. Jiang, Z., Hunt, J. V., and Wolff, S. P. (1992) *Anal. Biochem. 202*, 384−389.
8. Kahn, K. Ph.D. Thesis, Department of Biochemistry, University of Missouri, Columbia, 1998.
9. Sarma, A. D., and Tipton, P. A. (2000) *J. Am. Chem. Soc. 122*, 11252−11253.
10. Carter, J., and Wells, J. A. (1988) *Nature 332*, 564−568.
11. Berger, E., Arabshahi, A., Wei, Y., Schilling, J. F., and Frey, P. A. (2001) *Biochemistry 40*, 6699−6705.
12. Kleywegt, G. J. (1999) *J. Mol. Biol. 285*, 1887−1897.
13. Nar, H., Huber, R., Meining, W., Schmid, C., Weinkauf, S., and Bacher, A. (1995) *Structure 3*(5), 459−466.
14. Hennig, M., D'Arcy, A., Hampele, I. C., Page, M. G., Oefner, C., and Dale, G. E. (1998) *Nat. Struct. Biol. 5*(5), 357−362.
15. Ploom, T., Thony, B., Yim, J., Lee, S., Nar, H., Leimbacher, W., Richardson, J., Huber, R., and Auerbach, G. (1999) *J. Mol. Biol. 286*(3), 851−860.
16. Ploom, T., Haussmann, C., Hof, P., Steinbacher, S., Bacher, A., Richardson, J., and Huber, R. (1999) *Structure Fold. Des. 7*(5), 509−516.
17. Lu, G. (2000) *J. Appl. Crystallogr. 33*, 176−183.

BI027377X